

Copyright Warning & Restrictions

The copyright law of the United States (Title 17, United States Code) governs the making of photocopies or other reproductions of copyrighted material.

Under certain conditions specified in the law, libraries and archives are authorized to furnish a photocopy or other reproduction. One of these specified conditions is that the photocopy or reproduction is not to be “used for any purpose other than private study, scholarship, or research.” If a user makes a request for, or later uses, a photocopy or reproduction for purposes in excess of “fair use” that user may be liable for copyright infringement,

This institution reserves the right to refuse to accept a copying order if, in its judgment, fulfillment of the order would involve violation of copyright law.

Please Note: The author retains the copyright while the New Jersey Institute of Technology reserves the right to distribute this thesis or dissertation

Printing note: If you do not wish to print this page, then select “Pages from: first page # to: last page #” on the print dialog screen

The Van Houten library has removed some of the personal information and all signatures from the approval page and biographical sketches of theses and dissertations in order to protect the identity of NJIT graduates and faculty.

ABSTRACT

Fingerprint Pattern Recognition for Medical Uses

**by
Feng You**

The purpose of my research is to provide a method to automatically classify fingerprints into three subgroups: *whorl*, *loop* and *arch*, which can help medical scientists to study the relationship between fingerprint patterns and medical disorders. In the research, two different kinds of approaches were developed. The first one is performing pattern recognition in the frequency domain, which uses the feature of Fourier spectrum. That is, prominent peaks in the spectrum give the principal direction of fingerprint patterns. Using the above feature, we can obtain the principal direction of every subregion, after which the pattern of the whole image can be determined. The other approach is in space domain, a procedure which uses chain code to compute the changing direction of every ridge. The frequency domain approach allows one to classify whorl faster and is less sensitive to the quality of fingerprint image, but it does not easily allow for the classification of arch and loop when triradii areas are too small. The space domain approach can classify the above three patterns more accurately, but is much slower and more sensitive to fingerprint quality, especially the quality of triradii areas.

**FINGERPRINT PATTERN RECOGNITION
FOR MEDICAL USES**

**by
Feng You**

**A Thesis
Submitted to the Faculty of
New Jersey Institute of Technology
in Partial Fulfillment of the Requirements for the Degree of
Master of Science**

Biomedical Engineering

January, 1993

APPROVAL PAGE

Fingerprint Pattern Recognition for Medical Uses

Feng You

12/18/92

Dr. Yun-Qing Shi, Thesis Advisor
Assistant Professor of Electrical Engineering, NJIT

12/18/92

Dr. David Kristol, Committee Member
Professor of Chemistry, Director and Graduate Advisor of Biomedical
Engineering and Director of the Center for Biomedical Engineering, NJIT

12/18/92

Dr. Timothy N. Chang, Committee Member
Assistant Professor of Electrical Engineering, NJIT

BIOGRAPHICAL SKETCH

Author: Feng You

Degree: Master of Science in Biomedical Engineering

Date: January 1993

Date of Birth:

Place of Birth:

Graduate and Undergraduate Education:

- Master of Science in Biomedical Engineering
New Jersey Institute of Technology, Newark, NJ, 1993
- Bachelor of Engineering in Biomedical Engineering
Department of Automation
University of Electrical Science and Technology of China

Major: Biomedical Engineering

This thesis is dedicated to
my dear parents

ACKNOWLEDGEMENT

The author would like to express his sincere gratitude to his advisor, Dr. Yun Q. Shi, for his guidance, support, kindness and encouragement throughout the research work.

Special thanks to Professor David Kristol and Professor Timothy Chang for serving as members of the committee. Dr. Kristol's financial support for this work is also appreciated.

The author also want to thank Mr. Jingning Pan and Mr. Zhu Liu for their assistance in using DATACUBE device.

TABLE OF CONTENTS

Chapter	Page
1 INTRODUCTION	1
2 FINGERPRINT PATTERN CONFIGURATIONS	3
3 FINGERPRINTING METHODS	6
3.1 Ink-and-roll Method	6
3.2 Transparent Adhesive Tape Method	7
3.3 Photographic and Live Scan Methods	7
3.4 Computer Input of Fingerprints	8
4 FREQUENCY DOMAIN APPROACHES	10
4.1 Spatial Fourier Transform of Fingerprint	11
4.2 Single Region Analysis	14
4.3 Multiregion Analysis	14
5 SPACE DOMAIN APPROACHES	22
5.1 Conversion and Thinning	22
5.2 Ridge Following and Chain Code	24
6 EPILOGUE	28
APPENDIX	29
REFERENCES	35

LIST OF FIGURES

Figure	Page
2.1 Arch	4
2.2 Loop	4
2.3 Whorl	4
2.4 Double Loop Whorl	4
3.1 Fingerprint Input System	9
4.1 Fingerprint and its Frequency Spectrum Image	12
4.2 Whorl and Its $S(\theta)$ Plot	15
4.3 Loop and Its $S(\theta)$ Plot	15
4.4 Arch and Its $S(\theta)$ Plot	15
4.5a Arch	17
4.5b Arch $S(\theta)$ Array Analysis	18
4.6a Loop	17
4.6b Loop $S(\theta)$ Array Analysis	19
4.7a Whorl	17
4.7b Whorl $S(\theta)$ Array Analysis	20
4.8a Double Loop	17
4.8b Double Loop $S(\theta)$ Array Analysis	21
5.1 Whorl and Its Line Image	26
5.2 Loop and Its Line Image	26
5.3 Arch and Its Line Image	27
5.4 Double Loop and Its Line Image	27

CHAPTER 1

INTRODUCTION

Fingerprints are a kind of genetic markers which carry a great deal of genetic informations. Fingerprints have been studied for many years in order to discover the relationship between fingerprint patterns and some medical disorders such as breast cancer. In some studies, fingerprints need to be classified into subgroups. Currently, this kind of work should be done by trained technicians because there is no computer that can automatically do the job.

Dr. Murray H. Seltzer, University of Medicine and Dentistry of New Jersey, and some other doctors have been doing research to evaluate the relationship between fingerprint patterns and breast cancer for many years. Their research indicates that the presence of 6 or more whorls out of 10 possible fingers proved to be useful as a marker of women either at increased risk for breast cancer or already afflicted with the disease. To classify the prints, they had to get the ink-and-roll cards and send them to FBI which has technicians and equipments required to do this job. It is very inconvenient. And it is difficult to get a large enough set of fingerprints that they need because of the need to obtain the persons' permission to print their fingerprints. So they need a device that can classify fingerprints automatically and can input fingerprints directly without using the traditional ink-and-roll cards.

In my research, I used two approaches, frequency domain approach and space domain approach, to classify the fingerprints. In the frequency domain method, I cut a fingerprint image into several subregions, for example, 4 subregions or 9 subregions. By using the feature of Fourier spectrum that prominent peaks in the spectrum give the principal direction of fingerprint patterns, I can obtain the main direction of every subregion, then determine the pattern

of the whole image. This approach can classify *whorl* faster and is less sensitive to fingerprint quality, but it is difficult to classify *arch* and *loop* when triradii areas are too small.

In space domain method, I convert the fingerprint image into binary line image using thresholding and thinning techniques. Then by using the chain code to compute the direction changes of every ridge, the pattern of the image can then be determined. The space domain approach can classify the above three pattern more accurately, but is much slower and more sensitive to fingerprint quality, especially the quality of triradii areas.

Another problem is how to obtain fingerprint images. As mentioned above, to get an accurate result in the space domain, the image quality is very important. The traditional ink-and-roll method usually gives poor quality prints, and it is inconvenient. Recently, three kinds of fingerprinting machines called *live-scan* systems have become available. Using these systems, fingerprint images can be captured and translated into binary code automatically. And it is quick and accurate. These machines are currently made for law enforcement agencies, but they can be used in the medical research, too.

CHAPTER 2

FINGERPRINT PATTERN CONFIGURATIONS

In 1892, Galton divided ridge pattern into three groups: *arches*, *loops*, and *whorls*. Henry's classification (1937)[5] is only slightly different from Galton's in definition of whorls. Although there are many subclassifications, my research is concentrated on classifying fingerprints into these three groups because it is the most useful classification in medical diagnosis.

Arch (Figure 2.1) is the simplest pattern. It is formed by a series of more or less parallel ridges, which traverse the pattern area and form curves that are concave approximately. Sometimes the curve is gentle; sometimes it swings more sharply so that it may also be designated as a low or high arch, respectively. The arch pattern is subdivided into two types: *simple arch* and *tented arch*. The simple one is composed of ridges that cross the fingertip from one side to the other without recurving. If the ridges meet at a point so that their smooth sweep is interrupted, a tented arch is formed. The point of confluence is called a triradius (FBI call it delta) because ridges usually radiate from this point to three different directions. Sometimes, it may simulate a loop or even a much reduced whorl.

Loop (Figure 2.2) is the most common pattern. In this configuration, a series of ridges enters the pattern area on one side of the digit, recurves abruptly, and leaves the pattern area on the same side. If the ridge opens on the ulnar side, the resulting loop is termed an *ulnar loop*, whereas if it opens toward the radial margin it is called *radial loop*. A loop has a single triradius. It is usually located laterally on the fingertip and always on the side where the loop is closed.

A *Whorl* (Figure 2.3) in Galton's classification is any ridge configuration with two or more triradii. One is on the radial and the other on the ulnar side of the pattern. Henry limited the designation of "whorl" to those configurations having ridges that actually encircle a core. He called more complex pattern as *composites*. The ridges in a *simple whorl* are commonly arranged as a succession of concentric rings or ellipses. Such patterns are described as *concentric whorls*. Another configuration spirals around the core in either a clockwise or counterclockwise direction. This pattern is called a *spiral whorl*. Sometimes, both circles or ellipses and spirals are present in the same pattern.



Figure 2.1 Arch



Figure 2.2 Loop



Figure 2.3 Whorl



Figure 2.4 Double Loop Whorl

A *central pocket whorl* is a pattern containing a loop within which a smaller whorl is located. Another type is composed of interlocking loops, which may form either a *lateral pocket loop* or a *twin loop* pattern. Each has two triradii and according to Galton's classification, it is a whorl. These two types are normally called *double loop whorls* (Figure 2.4).

Complex patterns, which cannot be classified as one of the above patterns, are called *accidentals*. They represent a combination of two or more configurations, such as a loop and a whorl, triple loops, and other unusual formations.

CHAPTER 3

FINGERPRINTING METHODS

Several methods described in the following have been designed primarily to obtain fingerprints for dermatoglyphic analysis. Most of them cannot directly get a binary image file which can be used by computers, so some techniques, which have also been described in this chapter, are needed to transfer the fingerprint images into binary files.

3.1 Ink-and-Roll Method

As one of the best known and most widely used fingerprinting methods, the ink-and-roll method is the standard method used by law enforcement agencies for identification. It utilizes printer's ink, a roller, a glass or metal inking slab, a sponge rubber pad, and good quality paper, preferably with a slightly glazed surface.

A small amount of ink is placed on the inking slab and spread with the roller into a thin and even film. The area to be printed is pressed against the slab, taking care of that the whole area to be printed is covered with the ink. A firm surface is used under the sheet of paper on which the inked finger is pressed. The optimal amount of ink and pressure needed to obtain satisfactory prints is learned with a little practice. However, because these two factors are crucial for successful printing, this method is not suitable for use with uncooperative children and those with very fine ridges. The fingerprint images obtained by this method are sometimes not good enough for computerized pattern recognition. And they need to be convert to binary images.

3.2 Transparent Adhesive Tape Method

This method requires a transparent cellulose tape and white or pale yellow chalk. After the skin has been cleaned with ether, the fingertips are rubbed with chalk and a piece of tape is then placed over the area with the adhesive side against the skin. Light pressure is applied and the strip is then carefully removed. The chalk dust that adhered to the tape thus records the ridge detail.

Several modifications of the above method use different materials instead of chalk. These materials include India ink, standard ink or carbon paper. The powdered carbon-transparent tape method is very inexpensive, rapid and easy to use with all types of patient, including newborns. Prints are invariably clear and not smudged. They can be preserved for an indefinite time. But it is also not ready for computer to recognize.

3.3 Photographic and Live Scan Methods

The photographic method is based on the principle of frustrated total internal reflection which occurs when an object is pressed against a prism. The magnified image is photographed by a polaroid camera. The procedure is clean, because no ink is required, and the clarity of the print is not disturbed by applying pressure. This is an important factor because, with the ink method, it is difficult to ensure uniform, gentle pressure required for successful printing. The prints obtained by this method are very clear, but only areas in direct contact with the rigid surface of a prism can be photographed.

Live scan method uses a similar principle. In live-scan electronic fingerprinting, a finger is placed on a glass plate and its image captured with a video scanner at a precise oblique angle. As the finger is rolled across the plate, the computer builds an image over time, and the image is digitized according to its light intensity into binary computer image file. There are

three kinds of live-scan systems, two of them use the above-mentioned video optical devices to capture the fingerprint image, the other uses a different optical device and a U-shaped platen. Its sensor moves around the platen instead of rolling fingers.

There are other slight differences among these machines. One of them has live video feedback so the operator can see the finger on a monitor as it is rolled. The other two replay the captured images a second later.

The live scan method has two advantages. First, it gives clear fingerprint image, the reason is the same as the photographic method. Second, the images are already in a binary file format which can be used directly by computers. This is much faster than any traditional method. The only disadvantage is that the device is very expensive, costing up to \$60,000.

3.4 Computer Input of Fingerprints

The prints obtained with all the above methods except the live scan method need to be converted into binary computer files. There are several kinds of image input devices. For examples, the flying-spot scanner, video camera, even that used in fax machines.

In my research, I used a CCD video camera, a DATACUBE MaxVideo system and a SUN workstation to digitize the roll-and-ink cards I obtained from the Newark Police Department. The MaxVideo system includes many function modules like DIGIMAX, MAX-SCAN and MAX-SP, etc. This system is supported by MaxWare software, written in "C". Each MaxVideo board comes with its own MaxWare package. This includes a complete library of primitive functions, a device driver, hardware interface instructions, and an interactive library of Hardware Access Tools to control every hardware function on each board.

The most important module for my work is MAX-SCAN module. This is a versatile, asynchronous digitization module which accommodates the acquisition of non RS-170 video data and other types of signals from virtually any type of sensor. It has a 16-bit digital input port. It operates at data rates up to 10 MHz and handles any size video line up to 4092 pixels. It has many sophisticated DSP and data correction features not found in other digitization modules. By using above devices, each fingerprint is converted into a 512×512 8-bit GRAY format computer file which can be used by computers.

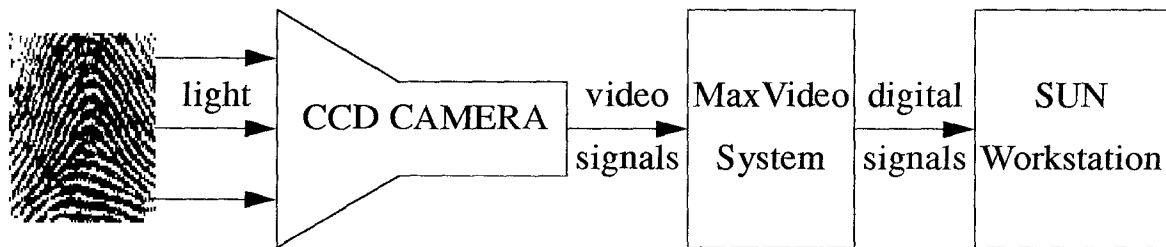


Figure 3.1 Fingerprint Input System

CHAPTER 4

FREQUENCY DOMAIN APPROACHES

Frequency spectrum is ideally suited for describing the directionality of a periodic or almost periodic two-dimensional pattern in an image. The global texture patterns, while being easily distinguishable as concentrations of high-energy bursts in the spectrum, are generally quite difficult to detect using spatial methods because of the local nature of these techniques.

In my work, I have used an image and signal processing software package, Khoros, to do preprocessing. Khoros, which runs under the X Windows system, is a software environment for research in the use of visual programming as a tool for software development for scientific visualization. The Khoros infrastructure consists of several layers of interacting subsystems. A user interface development system (UIDS) combines a high-level user interface specification with methods of software development and maintenance that are embedded in a code generation tool set. An interoperable data exchange format (VIFF) and algorithm library contain the application specific layer. The current library of over 260 routines has been developed to facilitate research in image processing, signal processing, pattern recognition, remote sensing, machine vision, and geographic information systems. Khoros is also a valuable teaching tool for signal and image processing. The routines I have used including 2-D FFT, 2-D Plot, editimage, and image format conversion programs, etc.

4.1 Spatial Fourier Transform of Fingerprint

The two-dimensional discrete Fourier transform (2-D DFT) pair is given by the following equations:

$$F(u, v) = \frac{1}{MN} \sum_{x=0}^{M-1} \sum_{y=0}^{N-1} f(x, y) e^{-j2\pi(\frac{ux}{M} + \frac{vy}{N})} \quad (4.1-1)$$

for $u=0, 1, 2, \dots, M-1, v=0, 1, 2, \dots, N-1$, and

$$f(x, y) = \sum_{u=0}^{M-1} \sum_{v=0}^{N-1} F(u, v) e^{j2\pi(\frac{ux}{M} + \frac{vy}{N})} \quad (4.1-2)$$

for $x=0, 1, 2, \dots, M-1, y=0, 1, 2, \dots, N-1$.

In my application, I used square array images. So $M=N$ and

$$F(u, v) = \frac{1}{N^2} \sum_{x=0}^{N-1} \sum_{y=0}^{N-1} f(x, y) e^{-j2\pi\frac{ux+vy}{N}} \quad (4.1-3)$$

for $u, v=0, 1, 2, \dots, N-1$, and

$$f(x, y) = \sum_{u=0}^{N-1} \sum_{v=0}^{N-1} F(u, v) e^{j2\pi\frac{(ux+vy)}{N}} \quad (4.1-4)$$

for $x, y=0, 1, 2, \dots, N-1$.

By using Equation (4.1-3) we can get the Fourier spectrum (Figure 4.1b) of a fingerprint image (Figure 4.1a). It is the most useful feature of the spectrum for fingerprint texture description in my work. That is the prominent peaks in the spectrum give the principal direction of the texture patterns. Because the spectrum image is symmetric about the origin, only half of the frequency plane needs to be considered.



Figure 4.1a Fingerprint Image

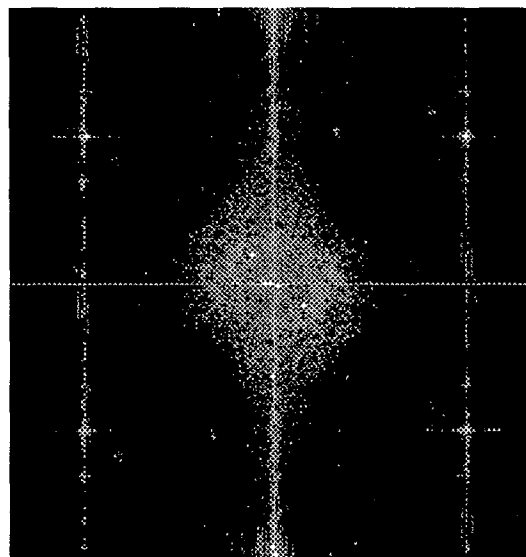


Figure 4.1b Frequency Spectrum Image

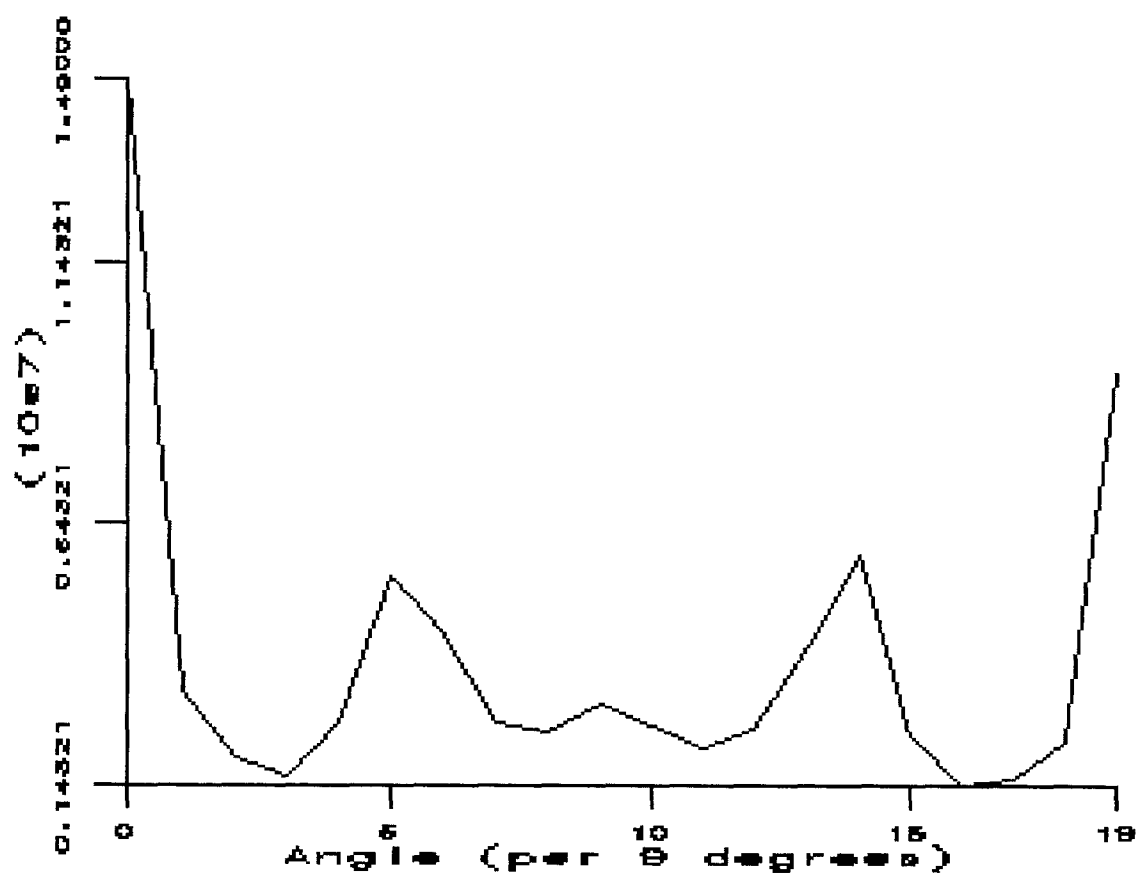


Figure 4.1c $S(\theta)$ Plot of Above Spectrum Image

To use the above feature to classify the fingerprint patterns, we can express the spectrum in polar coordinates to yield a function $S(r, \theta)$, where S is the spectrum function and r and θ are the variables in this coordinate system. Then, in each direction θ , we can consider $S(r, \theta)$ as a one-dimensional function $S(r)$. Similarly, for each frequency r , $S_r(\theta)$ is a one-dimensional function. Analyzing $S_\theta(r)$ for a fixed value of θ yields the behavior of the spectrum (e.g., the presence of peaks) along a radial direction from the origin, while analyzing $S_r(\theta)$ for a fixed value of r yields the behavior along a circle centered at the origin.

A more global description is obtained by integrating (summing for discrete variables) these functions, as follows:

$$S(r) = \sum_{\theta=0}^{\pi} S_{\theta}(r) \quad (4.1-5)$$

and

$$S(\theta) = \sum_{r=0}^R S_r(\theta) \quad (4.1-6)$$

where R is the radius of a circle centered at the origin. For a $N \times N$ spectrum, R is typically chosen as $N/2$.

The results of Equations (4.1-5) and (4.1-6) constitute a pair of values $[S(r), S(\theta)]$ for each pair of coordinates (r, θ) . By varying these coordinates, we can generate two one-dimensional functions, $S(r)$ and $S(\theta)$ (Figure 4.1c), that constitute a spectral-energy description of texture for an entire image or region under consideration. Furthermore, we can compute descriptors of these functions themselves in order to characterize their behavior in a quantitative manner.

For a fingerprint image, the locations of peaks in $S(r)$ represent width and distance of ridges. They are not very useful in my research. The most important descriptors are the locations of the peaks and their values in $S(\theta)$, which give the major directions and their relationships of the image.

4.2 Single Region Approach

In this approach we can get the global directions of the entire fingerprint image. We assume the polar coordinates start from right to left of the origin (from 0° to a little bit less than 180°). That is 0 to 19 (per 9 degrees) in all of the $S(\theta)$ plots. The 0° represents horizontal direction and 90° represents vertical direction. Due to the nature of fingerprint images (there are many ridge lines that have a horizontal direction component), there will always be two major peaks near 0° and 180° .

For many of the whorls, there are two major peaks in $S(\theta)$ with approximate values around 45° and 135° , and a little peak around 90° (Figure 4.2b). For many of the loops, there are also two peaks (may or may not with much different values) around 45° and 135° , and a little peak around 90° (Figure 4.3b) too. For arches (except high arch), there are no peaks around 90° .

Because single region approach can only give major directions of the entire image, it cannot classify fingerprint patterns clearly. But we can use the same principle to try multiregion approaches which can give us more details of the fingerprint.

4.3 Multiregion Approaches

To get a more detailed analysis of the fingerprints, we can divide an entire fingerprint image into several subregions, for example, 2×2 or 3×3 . As we can see, the more subregions, the higher precision. But the number of



Figure 4.2a Whorl

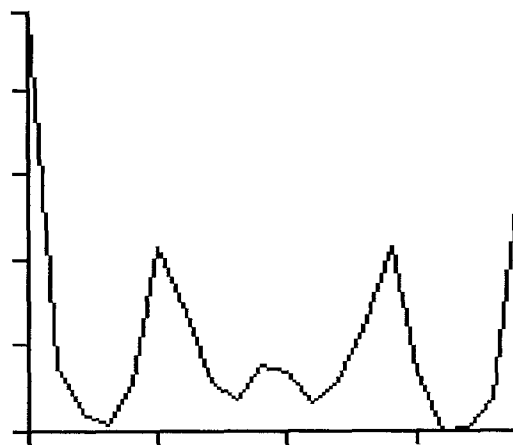


Figure 4.2b $S(\theta)$ of Whorl



Figure 4.3a Loop

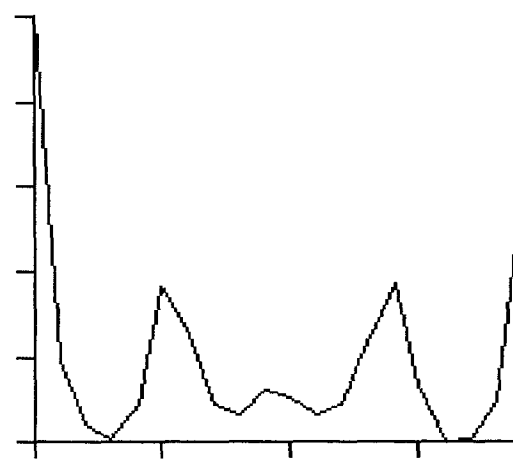


Figure 4.3b $S(\theta)$ of Loop



Figure 4.4a Arch

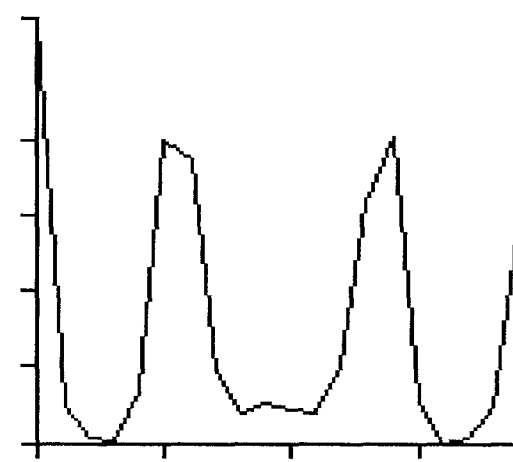


Figure 4.4b $S(\theta)$ of Arch

subregions is limited by the resolution of the image. And the more subregions, the more complex the algorithm is, and the more time the procedure needs. So in my research, I chose 3×3 subregions for images of 384×384 that were resulted from cutting off images of 512×512 . In my analysis of $S(\theta)$ plots patterns, I define the subregion number from 1 to 9 according the sequence of left to right and top to bottom.

In the following figures of $S(\theta)$ plots, we can find the difference among three fingerprint patterns, except when the triradius area is too small. In almost all kinds of whorls with large or middle center region, including concentric whorls, spiral whorls and double loop whorls, we expect to see V-shape patterns in the set of $S(\theta)$ plots. That means that for 3×3 subregions, there is at least one pair of horizontally connected regions in the lower 2 layers; one has a major direction around 45° and another around 135° . These looks like a V. That is because the ridge lines between and above (but near) the two triradii of whorl are proximate concave with upward opens. There is no V-shape pattern in loops and arches, so this can be a feature to differ whorls from other two patterns.

The difference in the set of $S(\theta)$ plots between loops and arches cannot be seen easily. In a loop, the ridges near and above the triradius have vertical or almost vertical direction. But in arches (except tented arches), there are no such ridges. So if the subregion is small enough, or the triradius region is large enough, we can see that at least one subregion has a major vertical direction in a loop.

An alternate method involves using three connected small windows to scan over the entire image to find the triradii area. These three windows compose a triangle. In the area near the triradii, ridge lines change to three directions. When these window move to an area, we can compute the $S(\theta)$ of them

to find the major direction of each subregion. If the three directions point to the center of the three windows, we can then determine that this area is a triradius area. Like Galton's definition, we can say that no triradius means arch, one triradius means loop, and whorl has two or more triradii. This will simplify the classification of fingerprint patterns. But this approach needs high resolution and high quality images, which I don't have now.



Figure 4.5a Arch



Figure 4.6a Loop



Figure 4.7a Whorl



Figure 4.8a Double Loop

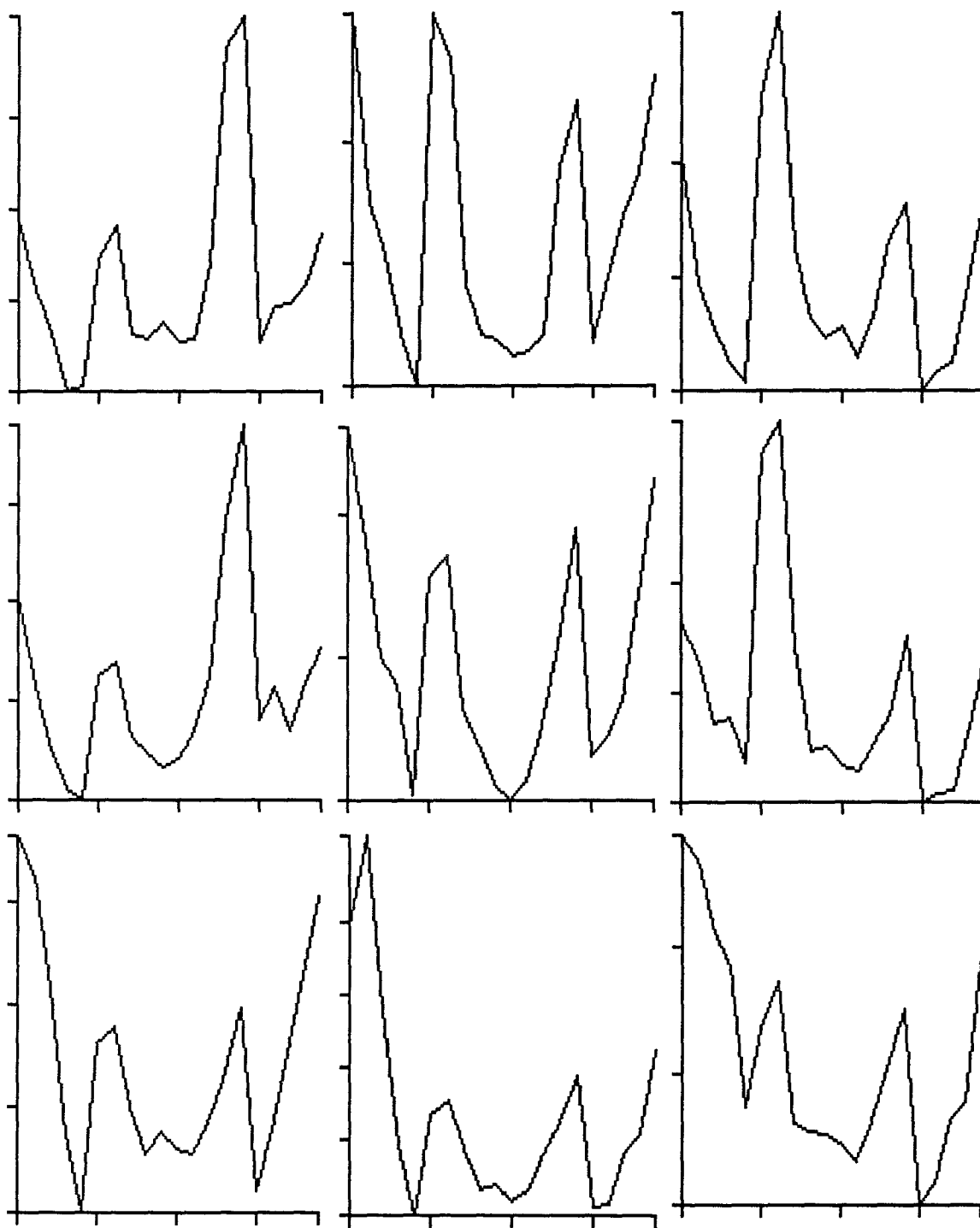


Figure 4.5b Arch $S(\theta)$ Array Analysis. There is no V-shape pattern and we can hardly see peaks around 90° because there is no vertical ridge lines.

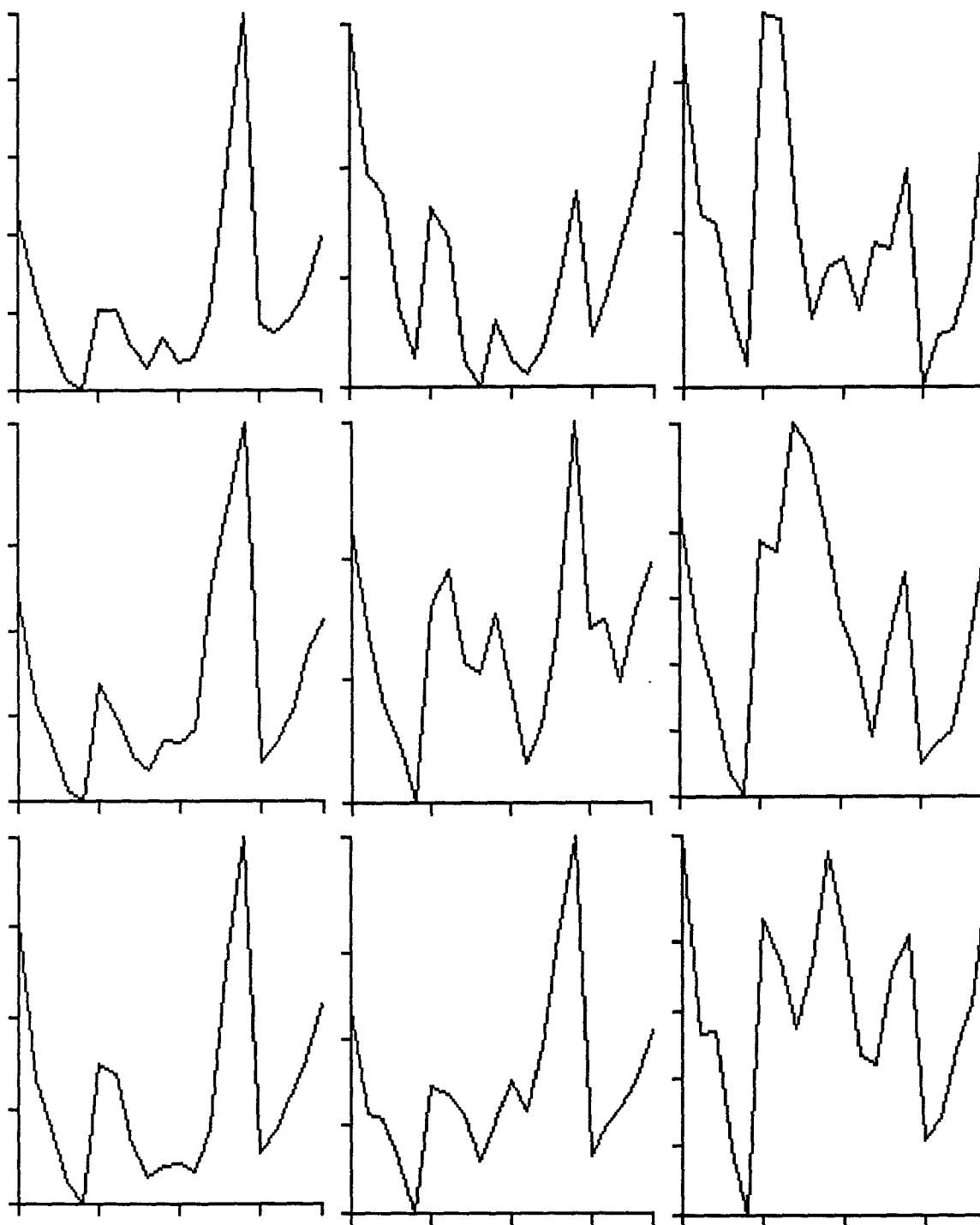


Figure 4.6b Loop $S(\theta)$ Array Analysis. As we can see, there is no V-shape pattern. But plot 9 (the right bottom corner) shows there is a major direction around 90° and has two peaks around 45° and 135° . That because this is a triradius region.

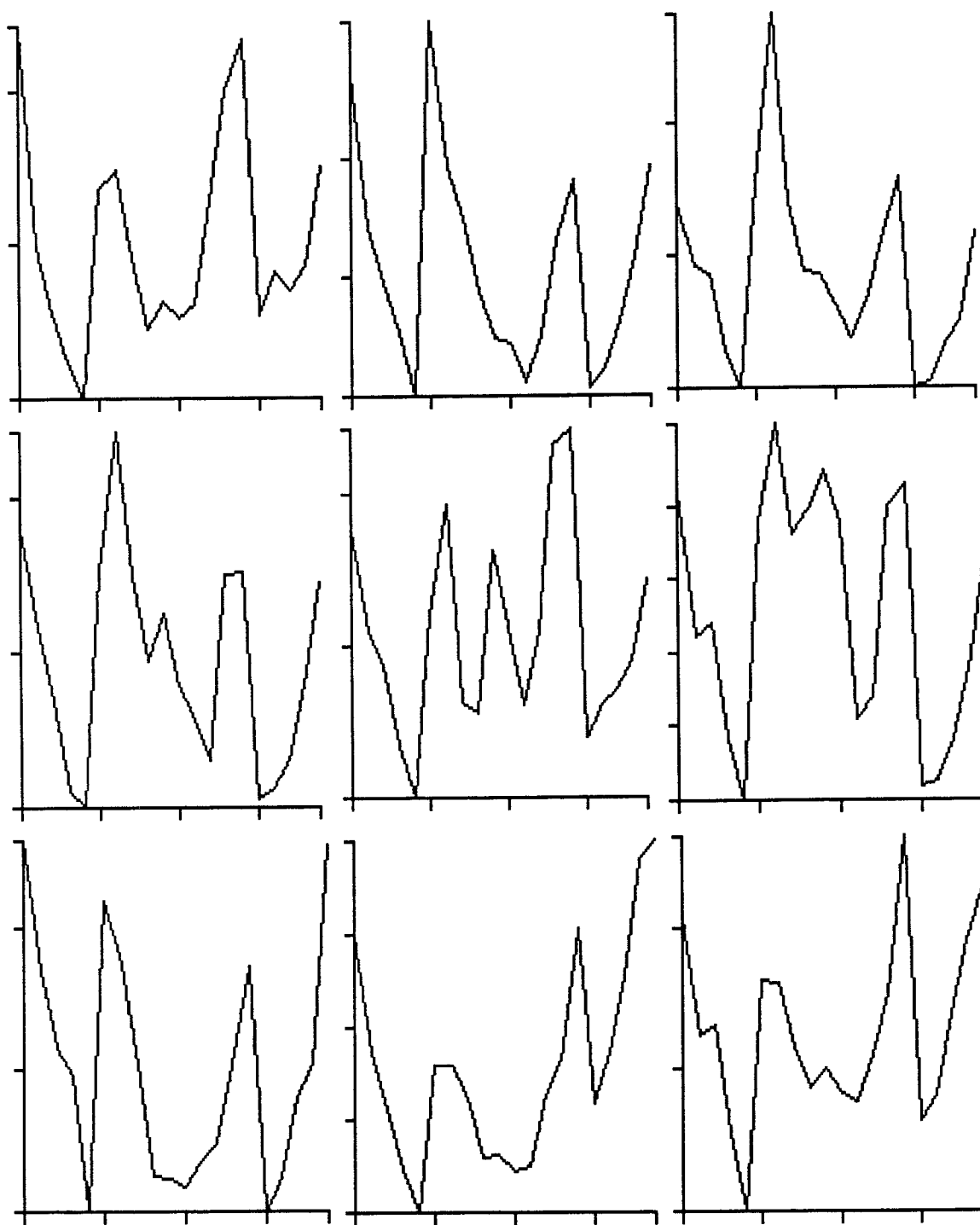


Figure 4.7b Whorl $S(\theta)$ Array Analysis. The plots 4 and 5, 7 and 8 compose two pair of V-shape pattern. So we can say it is a whorl.

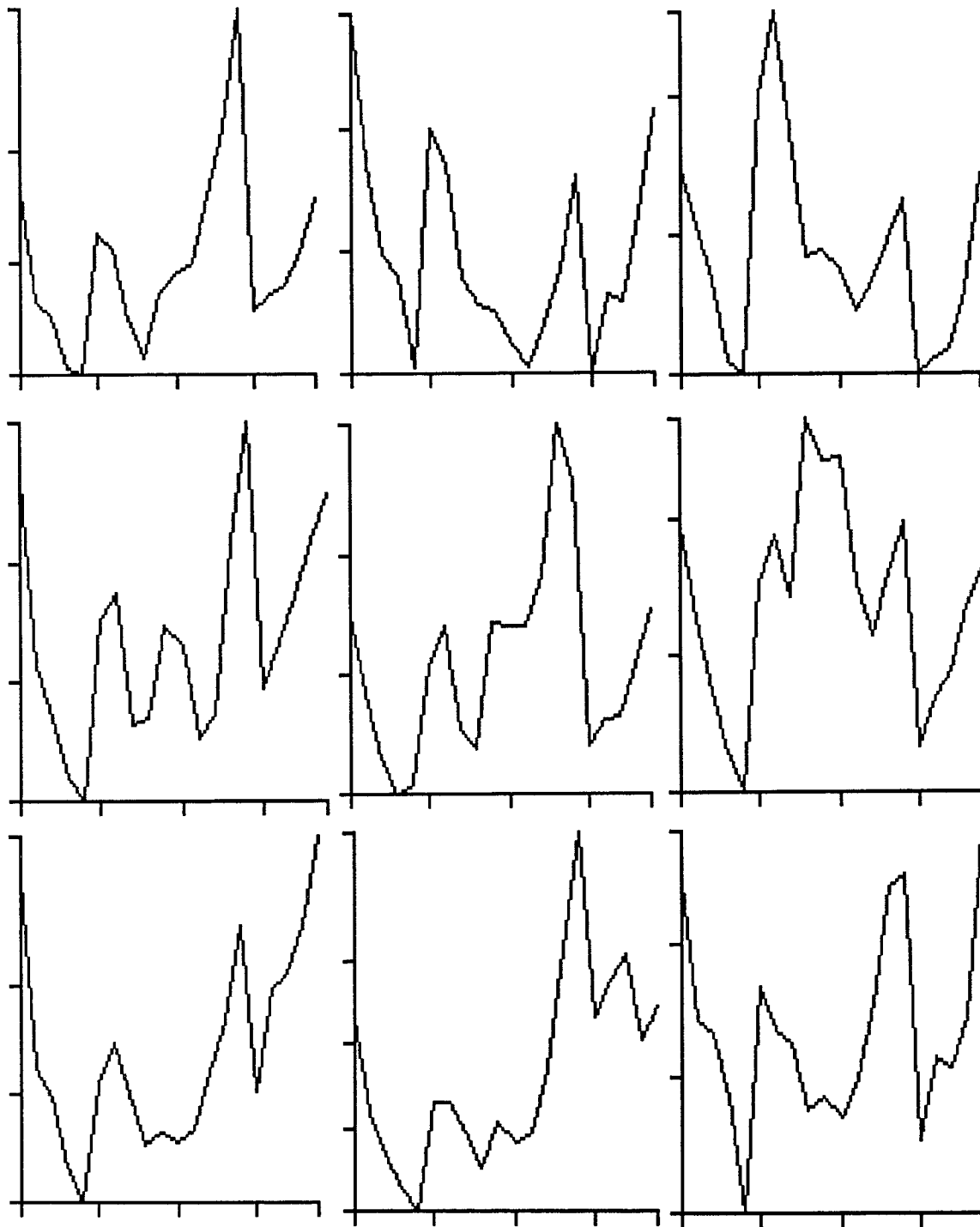


Figure 4.8b Double Loop $S(\theta)$ Array Analysis. The plot pattern of above double loop look like loop (without V-shape pattern). But plot 4 and 6 indicate there may be two triradii.

CHAPTER 5

SPACE DOMAIN APPROACHES

In the case of fingerprint with small triradius area, the frequency domain may not give good results. That because the frequency domain approach applies FFT which requires a relatively large area. So I used another approach, in space domain, to try to solve this problem. This approach is based on the reasoning that if we can find ridge lines which fit for the definitions of one of the three patterns, we can determine the fingerprint pattern definitely. Due to the nature of this spatial method, image quality is very important, and the algorithm is complex.

5.1 Conversion and Thinning

The first step of this approach is to convert an 8 bits grey level image into a binary image. Because the ridges and the valleys have very different grey level values, the threshold can be easily selected from some values between two peaks in the grey level histogram.

Then the binary ridge image should be thinned to an 8-connected line image. It is assumed that the ridge pixel value is “1”, and valley pixel value is “0”. The pixel bond as the sum of the bond weights between the center pixel and each of its neighbors. Each four-connected neighbor with “1” value has a bond weight of two, and each of other eight-connected neighbor with “1” value has a bond weight of one. By using the bond number, We can separated the pixels into several groups. Then I used a small odd-sized mask (3×3) to scan over the binary image. If the binary-valued pattern of the mask matched the state of the pixels under the mask (hit), then an output pixel in spatial correspondence to the center pixel of the mask was set to some desired binary

Table 5.1 Thinning Algorithm Hit Mask Patterns

Bond	Pattern							
4	0 1 0	0 1 0	0 0 0	0 0 0	0 0 1	1 1 1	1 0 0	0 0 0
	0 1 1	1 1 0	1 1 0	0 1 1	0 1 1	0 1 0	1 1 0	0 1 0
	0 0 0	0 0 0	0 1 0	0 1 0	0 0 1	0 0 0	1 0 0	1 1 1
5	0 1 1	1 1 0	0 0 0	0 0 0	1 1 0	0 1 0	0 0 0	0 0 1
	0 1 1	1 1 0	1 1 0	0 1 1	0 1 1	1 1 0	1 1 0	0 1 1
	0 0 0	0 0 0	1 1 0	0 1 1	0 0 0	1 0 0	0 1 1	0 1 0
6	1 1 1	1 1 0	0 0 0	0 0 1	1 0 0	0 0 0	0 1 1	1 1 1
	0 1 1	1 1 0	1 1 0	0 1 1	1 1 0	0 1 1	0 1 1	1 1 0
	0 0 0	1 0 0	1 1 1	0 1 1	1 1 0	1 1 1	0 0 1	0 0 0
6	1 1 0	0 1 1	0 0 1	1 0 0				
	0 1 1	1 1 0	0 1 1	1 1 0				
	0 0 1	1 0 0	1 1 0	0 1 1				
7	1 1 1	1 1 1	1 0 0	0 0 1				
	0 1 1	1 1 0	1 1 0	0 1 1				
	0 0 1	1 0 0	1 1 1	1 1 1				
8	0 1 1	1 1 1	1 1 0	0 0 0				
	0 1 1	1 1 1	1 1 0	1 1 1				
	0 1 1	0 0 0	1 1 0	1 1 1				
9	1 1 1	1 1 1	1 1 0	0 0 1	0 1 1	1 1 1	1 1 1	1 0 0
	0 1 1	1 1 1	1 1 0	1 1 1	0 1 1	1 1 1	1 1 0	1 1 1
	0 1 1	1 0 0	1 1 1	1 1 1	1 1 1	0 0 1	1 1 0	1 1 1
10	1 1 1	1 1 1	1 1 1	1 0 1				
	0 1 1	1 1 1	1 1 0	1 1 1				
	1 1 1	1 0 1	1 1 1	1 1 1				

state (in my work, “0”). For a pattern mismatch (miss), the output pixel was set to the opposite binary state (“1”). This technique is called Hit or Miss Transformations. The hit patterns are listed in Table 5.1. After I performed the above transformations over and over until all pixels in the image mismatch the hit pattern, I obtained the final line image.

Hit or miss morphological algorithms are often implemented in digital image processing hardware by a pixel stacker followed by a look-up table (LUT). This technique will accelerate the processing speed very much. But in my research, I only used a software algorithm instead.

5.2 Ridge Following and Chain Code

After we get the line image, we should do some work to “repair” the lines. That means to remove the short branches and link the short intervals, etc. For example, if a branch is less than 5 pixels in length (the number depends on the resolution of the image) from connection point, we can move it off. If two lines have similar directions and the two ends near each other (the distance between two ends is less than 5 pixels or so), we can connect them.

In my work, I used an alternative method to do the link. When finding an end, I computed the tangent direction near the end by using chain code. Then I searched along this direction (allowing a little bit tolerance) in a short distance to see if it can meet another end with similar direction.

The final step and the most important one is to determine the fingerprint pattern by using ridge following algorithm. If after the above steps we get a clear, connected ridge line image, we can compute the direction change of every ridge line in the image. When a line changes direction 360° or more, we can say it's a whorl by Henry's definition. If no line changes direction from one side to another, it should be an arch. Otherwise, it has at least one loop.

To classify loop and more complex patterns, we can compare the open direction of the lines. The direction of the opening of these line in simple loop should be unique. Other complex patterns can be determined by the method, too.

The most difficult problem is that the quality of fingerprint images may not be good enough to be applied by above algorithm. This approach requires that the entire image should be clear and ridge lines cannot have many intervals. In my research, I used a more simple approach to classify whorl, which is the most important one for the research of evaluating the relationship between fingerprint patterns and breast cancer. Because the ridge lines between two triradii are approximately concave with upward opening, we can just apply the ridge following algorithm to find these lines. That is, if we find out that a line changes its direction from slightly downward to slightly upward (the feature of concave segment with upward opening), we will say the pattern is a whorl. This only requires the lines running between triradii must be clear. That is the FBI's requirement of whorl on roll-and ink card.



Figure 5.1a Grey Level
Image of Whorl



Figure 5.1b Binary Line
Image of Whorl



Figure 5.2a Grey Level
Image of Loop



Figure 5.2b Binary Line
Image of Loop



Figure 5.3a Grey Level
Image of Arch



Figure 5.3b Binary Line
Image of Arch



Figure 5.4a Grey Level Image of
Double Loop



Figure 5.4b Binary Line Image of
Double Loop

CHAPTER 6

EPILOGUE

The problem of automatically classifying fingerprint patterns has not been solved to this time. According to the report of The New York Times [1], the Orincon Corporation in San Diego, California, is working on this puzzle with neural networks.

Neural Network is a new kind of technique in the artificial intelligence field. The neural networks have been installed in the sonar system of submarine to recognize sonar patterns. They filter the cacophony beneath the sea, permitting only sounds of "interest" to be displayed on sonar instruments. The Orincon Corporation, a military contractor, which has built sound-detecting neural networks for Navy since 1986, is trying to use the same technique to classify fingerprint patterns automatically. It plans to be among the companies competing for an F.B.I. award to build a prototype fingerprint pattern sorter.

The work I have done is trying some initial attempt for solving this problem. The result is not totally satisfactory, partly due to the poor quality of the fingerprint images that I used. The multiregion frequency domain approach is expected to get fine result in 8X8 or more array (I only try 5X5 as the largest array) if the entire image is very clear. And the algorithm is much simple compared to the time domain approach. Theoretically, the time domain ridge following algorithm will be the most precise one. But due to its requirement of high image quality, it still has difficulty in dealing with many real images; and it is complex in algorithm.

APPENDIX

Thinning Program

```
# include <stdio.h>
# include <math.h>
# define size 256
main (argc, argv)
int argc;
char *argv[];
{
    FILE *fp, *fp1, *fopen();
    char image[size][size];
    if (argc==1)
        printf("There is no input file.\n");
    else if (argc==2)
        printf("There is no output file.\n");
    else if ((fp=fopen(argv[1], "r"))==NULL)
        printf("Can't open %s\n", argv[1]);
    else {
        fp1=fopen(argv[2], "w");
        inputf(fp, fp1, image);
        thinning(image);
        outputf(fp1, image);
    }
}
```



```

inputf(fp, fp1, im)
char im[size][size];
FILE *fp, *fp1;
{
    int x, y, c;
    for (x=0; x<1408; x++)
        putc(getc(fp), fp1);
    for (y=0; y<size; y++)
        for (x=0; x<size; x++)
            im[x][y]=getc(fp);
    fclose(fp);
}
thinning(im)
char im[size][size];
{
    int x, y, s=1, b, b1, b2, a1, a2, a3, a4;
    char n1, n2, n3, n4, n5, n6, n7, n0;
    while (s==1){
        s=0;
        for (y=1; y<size-1; y++)
            for (x=1; x<size-1; x++){
                if (im[x][y]==1){
                    n0=im[x+1][y];
                    n1=im[x+1][y-1];
                    n2=im[x][y-1];
                    n3=im[x-1][y-1];
                    n4=im[x-1][y];

```

```

n5=im[x-1][y+1];
n6=im[x][y+1];
n7=im[x+1][y+1];
b1=n1+n3+n5+n7;
b2=n0+n2+n4+n6;
b=b1+b2+b2;
if(b==4){
    if(b2==2&&(n0==n2||n2==n4||n4==n6||n6==n0)){
        im[x][y]=0;
        s=1;
    }
    else if(b2==1){
        a1=n7+n0+n1;
        a2=n1+n2+n3;
        a3=n3+n4+n5;
        a4=n5+n6+n7;
        if (a1==3||a2==3||a3==3||a4==3){
            im[x][y]=0;
s=1;
        }
    }
}
else if(b==5&&b2==2){
    a1=n7+n0+n1;
    a2=n1+n2+n3;
    a3=n3+n4+n5;
    a4=n5+n6+n7;

```

```

    if(a1==0||a2==0||a3==0||a4==0)
        if(n0==n2||n2==n4||n4==n6||n6==n0){
im[x][y]=0;
s=1;
        }
    }
else if(b==6&&b2==2&&(n0==n2||n2==n4||n4==n6||n6==n0)){
    a1=n0+n1+n2;
    a2=n2+n3+n4;
    a3=n4+n5+n6;
    a4=n6+n7+n0;
    if(a1==0||a2==0||a3==0||a4==0){
        im[x][y]=0;
        s=1;
    }
}
else if(b==7){
    a1=n0+n1+n2;
    a2=n2+n3+n4;
    a3=n4+n5+n6;
    a4=n6+n7+n0;
    if(a1==0||a2==0||a3==0||a4==0){
        im[x][y]=0;
        s=1;
    }
}
else if (b==8){

```

```

    a1=n7+n0+n1;
    a2=n1+n2+n3;
    a3=n3+n4+n5;
    a4=n5+n6+n7;
    if (a1==0||a2==0||a3==0||a4==0){
        im[x][y]=0;
        s=1;
    }
}
else if(b==9){
    a1=n7+n0+n1;
    a2=n1+n2+n3;
    a3=n3+n4+n5;
    a4=n5+n6+n7;
    if (a1==1||a2==1||a3==1||a4==1){
        im[x][y]=0;
        s=1;
    }
}
else if(b==10&&(n0==0||n2==0||n4==0||n6==0)){
    im[x][y]=0;
    s=1;
}
}
}
}
}

```

```
outputf(fp1, im)
char im[size][size];
FILE *fp1;
{
    int x, y;
    for (y=0; y<size; y++)
        for (x=0; x<size; x++)
            putc(im[x][y], fp1);
    fclose(fp1);
}
```

REFERENCES

1. Adelson, A. "Faster, More Accurate Fingerprint Matching." *The New York Times*, October 11, 1992
2. Gonzalez, R. C., and P. Wintz. "Digital Image Processing, Second Edition." *Addison-Wesley Publishing Company*.
3. "Khoros User's Manual." *University of New Mexico* (1991).
4. "MaxVideo System Manual." *DATAcube Company* (1991).
5. Schaumann, B. and M. Alter. "Dermatoglyphics in Medical Disorders." *Spring-Verlag* (1976).
6. Seltzer, M. H., C. C. Plato, and K. M. Fox. "Dermatoglyphics in the Identification of Women Either With or at Risk for Breast Cancer." *American Journal of Medical Genetics* 37 (1990):482-488.